Immigration and changing heat exposure disparities in the United States since 1990

Abbie Robinson
The Pennsylvania State University

Abstract

The population exposed to excessive heat is driven by both climate and demographic dynamics, yet the relative impacts of each component remain unclear. As public and policy attention to heat-related risks increases, understanding the respective roles of environmental and population change is critical to identifying disparities in exposure. Drawing on three decades of geolocated census and high-resolution climate data, I use demographic decomposition methods to address two research objectives. First, I estimate how shifts in local temperature and the geographic distribution of the (non)immigrant population contribute to changes in heat exposure in the continental United States from 1990 to 2020. Second, I evaluate heterogeneity in these changes by spatial and demographic contexts (i.e., metropolitan status, United States census division, world region of origin). I find that higher heat exposure among the foreign- than native-born population is attributable to both rising temperatures and population redistribution, with the dominant driver depending on whether the temperature metric reflects air temperatures or the physiological burden of heat and humidity. Importantly, however, I also detect meaningful regional and subpopulation differences in the contributions of each effect. With clear inequalities by nativity, this descriptive analysis underscores the importance of integrating local climate and demographic dynamics in environmental policies to more effectively address disparities in U.S. heat exposure.

Introduction

The extent of population exposure to warm temperatures is shaped by the interplay between climatic and demographic change. As calls for climate adaptation from policymakers and the public grow, understanding how population and environmental change contribute to heat exposure can help identify shifts in the magnitude and distribution of heat-related risks. Prior research has used decomposition as a demographic method to break down the aggregate change in observed heat exposure, examining a wide range of populations, including older adults in the United States, residents in some of the most populous regions globally (e.g., China, India), and urban dwellers across more than 13,000 cities (Carr et al., 2024; Park et al., 2020; Tuholske et al., 2021). No studies, however, have examined differences in heat profiles by nativity, leaving it unclear whether disparities between foreign- and U.S.-born populations are driven more by temperature change or population redistribution.

Decomposition, a core demographic technique, is a useful method for addressing this empirical gap by isolating the respective contributions of temperature and population effects on overall exposure in an intuitive manner. For the latter effect, previous research has documented that aging societies and urban growth serve as main contributors to changes in population heat exposure (Carr et al., 2024; Park et al., 2020; Tuholske et al., 2021). Demonstrating the utility of demographic decomposition, I extend the work of these studies by investigating three decades (1990-2020) of heat exposure by nativity status across the contiguous United States. The United

States provides a critical context for understanding patterns of heat exposure, as it remains one of the top destinations for international migration, with over 15 percent of the population being foreign-born (FitzGerald, 2022; Fong et al., 2022). Historical settlement areas (e.g., California, Texas, Florida), employment industries, and other social disadvantages (e.g., lack of health insurance) may further contribute to greater heat vulnerability among the immigrant population (Crowley et al., 2019; Flippen & Farrell-Bryan, 2021; Johnson & Lichter, 2019; Johnson & Winkler, 2015; Lichter & Johnson, 2009; Slesinski et al., 2025; Taylor et al., 2018).

To descriptively examine differences in heat exposure between foreign- and U.S.-born populations, I estimate how shifts in temperature and the respective spatial distribution of these populations have contributed to changes in exposure from 1990 to 2020. Because both temperature and population dynamics vary substantially across space and demographic groups, I then explore heterogeneity across key spatial and demographic dimensions (i.e., metropolitan status, U.S. census division, world region of origin. By examining variation in exposure across subpopulations and geographic contexts, this analysis clarifies how population and climatic processes jointly shape heat exposure in the United States. Using demographic decomposition, I further disentangle whether observed disparities stem from temperature changes, population shifts, or some combination of both, providing new insights into how immigrants experience heat relative to U.S.-born populations.

The remainder of this paper is structured as follows. First, I review existing research and outline the mechanisms motivating this analysis. Next, I detail the analytical strategy, followed by a presentation of the results. I then conclude with a discussion of key findings and broader policy implications. To summarize the main takeaways, immigrants have consistently experienced higher heat exposure than U.S.-born individuals since 1990. Demographic decomposition by nativity reveals that increases in exposure are driven by both warming temperatures and shifts in where populations live, with the relative contributions of these effects varying by exposure metric. Further analysis of spatial and demographic heterogeneity uncovers notable variation across U.S. census divisions, metropolitan status, and world regions of origin, highlighting important differences in heat exposure among immigrant subpopulations and across geographic regions. Consistent with prior research, these findings support the need for mitigation strategies that account for both demographic change and spatial warming patterns to support policy and programming responses to heat exposure in the United States.

Migration and heat stress

Migration and climate are two of the most politicized topics of global debate, and the complex interactions between population and climate factors have motivated a number of decomposition-focused investigations (Carr et al., 2024; Park et al., 2020; Tuholske et al., 2021). Carr et al. (2024), for example, examine the duality of population aging and rising heat in the United States, showing that higher temperatures drive exposure in historically colder regions, while aging populations increase heat susceptibility in the South. Next, Park et al. (2020) combine climate and population projections to find that summer warming in aged (65+) societies (e.g., the United States. and Europe) increases heat exposure, whereas the role of population aging largely contributes to exposure in India and sub-Saharan Africa. Extending this decomposition approach to city contexts, Tuholske et al. (2021) show that (1983-2016) urban warming drives exposure 52 percent higher than population growth, and spatial patterns of warming emphasize the need for place-based interventions (e.g., outdoor worker protection, cooling energy) to effectively address heat inequality. Together, these studies demonstrate how demographic decomposition can

disentangle the relative influence of temperature and demographic change on heat exposure across diverse contexts.

Drawing on of these empirical records, I expect change in (non)immigrant heat exposure to be explained by at least two factors. First, the climatic trend of warming temperatures contributes to how populations experience heat across a nation. According to the National Centers for Environmental Information, annual U.S. temperatures have increased by approximately 0.13 °C (0.23 °F) per decade since 1910 (National Oceanic and Atmospheric Administration, 2022), and nine of the ten warmest years have occurred since the late 1990s, indicating that U.S. temperatures are rising faster than the global rate of warming. Geographically, the greatest increases in temperature have been observed in the North and West, indicating place-specific variation in warming trends (United States Environmental Protection Agency, Climate Change Indicators: U.S. and Global Temperature 2024). These patterns highlight regions experiencing substantially faster warming than others, reinforcing spatial disparities in heat exposure and associated risks. As these hotspots continue to experience higher maximum temperatures and more frequent heat waves, ongoing and projected warming across the United States underscores the urgency for heat policies and adaptation strategies.

Second, changes in the geographic distribution and composition of a population—shaped in part by migration—play a key role in aggregate patterns of heat exposure across a country context. Migration decisions are influenced by multiple push (e.g., political instability, economic hardship, environmental change) and pull (e.g., employment, social network ties) factors that motivate U.S.-bound and internal movement (Flippen & Farrell-Bryan, 2021; Lichter & Johnson, 2009), and while immigrants are racially and ethnically diverse, scholars have given particular attention to the settlement patterns of Hispanics (Jessoe et al., 2018; Nawrotzki et al., 2013, 2015). Lichter & Johnson (2009), for instance, document a widening geographic dispersion of Hispanics across both established and new destinations. In 2000, nearly three-quarters of Hispanics resided in established destinations (e.g., California, Texas), even though these areas contained only about 29 percent of the total U.S. population. At the same time, Hispanic populations in new destinations grew substantially faster than in these gateway states—approximately five times faster during the 1990s and three times after 2000—pointing to the rapid spread of Hispanics into new regions such as the Midwest and South. Johnson and Winkler (2015) further expand on key signatures of U.S. migration, showing an inflow of young (under 50) Hispanic moves to nonmetropolitan, suburban and small metropolitan counties between 1950 and 2010. Immigrants of Asian and African origin have reflected a wider geographic dispersal in the United States as well (Flippen & Farrell-Bryan, 2021; Frey et al., 2005). Importantly, these mobility patterns suggest that migration may either increase or decrease population exposure to heat, further motivating this investigation.

Furthermore, migrant redistribution patterns such as these directly impact the demographic composition and growth of local economies. The dispersion of high- and low-skilled immigrants reflects the demand of labor markets, and studies document an increase in native-born White outmigration alongside foreign-born population growth (Flippen & Farrell-Bryan, 2021; Hall & Crowder, 2014). Latinos, often described as the as the demographic lifeline of rural America, have played a critical role in sustaining population growth through migration and higher fertility rates in many U.S. counties (Crowley et al., 2019; Johnson & Lichter, 2019; Johnson & Winkler, 2015). Their concentration in rural areas and outdoor occupations (e.g., agriculture, construction) not only supports local economies but may also increase vulnerability to hot working conditions (Zhang et al., 2016)

Beyond labor market dynamics, immigrant mortality risk may further impact foreign-born heat exposure. As evidence, Taylor et al. (2018) show that non-U.S. citizens (particularly of Hispanic ethnicity) have a higher likelihood of heat-related mortality compared to their US citizen counterparts. Other literature emphasizes broader rural disparities, as limited medical services and personnel complicate health access for remote populations (Burton et al., 2013; Jensen et al., 2020; Miller & Vasan, 2021). Given the challenges of social marginalization and structural inequalities expected to disproportionally impact immigrant populations, rising temperatures in counties where specific demographics are concentrated may further exacerbate heat-related disparities.

Objectives

I use demographic decomposition methods to address two research objectives centered on linkages between population change, warming, and heat exposure in the US. First, I estimate how shifts in temperature and the respective spatial distributions of the foreign- and U.S.-born populations have affected change in heat exposure across the contiguous United States since 1990. Second, I explore spatial and demographic heterogeneity, by metropolitan status, U.S. census divisions (i.e., Pacific, Mountain, West North Central, East North Central, New England, Middle Atlantic, West South Central, East South Central, and South Atlantic), and foreign-born world region of origin (i.e., Africa, Asia, the Americas, Europe, and Oceania).

Analytic Strategy

Data

I access census data (1990, 2000, 2020) from the National Historical Geographic Information System (NHGIS), extracted using IPUMS (Schroeder et al., 2025). IPUMS-NHGIS compiles and harmonizes time-series census data and summary tables (e.g., the American Community Survey) produced by the US Census Bureau across multiple geographic levels. For this study, I rely on county-level demographic data (n=3,108), with publicly available geographic entity codes that enable linkage to an (1) ambient temperature and (2) heat stress metric.

Using data from the Parameter-elevation Regressions on Independent Slopes Model (PRISM), I measure variation in ambient temperatures. With inputs from 10,000 weather stations, PRISM provides high spatial resolution (4 km) climate data products produced by Oregon State University, and these data are widely used in US population-environment research (Ahn et al., 2024; Albouy et al., 2016; Clark et al., 2024; Clay et al., 2021; DeVine et al., 2017; Nori-Sarma et al., 2022; Spangler et al., 2019; Winkler & Rouleau, 2021). PRISM's methodological rigor and consistent temporal coverage ensure reliable measurement of daily maximum temperature (Tmax) records, the air temperature metric used in this study.

Unlike shorter-term or more volatile metrics (e.g., anomalies), Tmax captures chronic heat exposure, reflecting the sustained ambient thermal conditions experienced by the US population over a daily exposure period. Measured consistently across time and space, and independent of a shifting baseline, Tmax provides a stable and comparable proxy for long-term air temperature. I expect Tmax to be a critical factor in the U.S. context, as historical records since the late 19th century document rising temperatures and climate models project higher annual temperatures nationwide, along with more frequent and intense heat events (Calvin et al., 2023) (Calvin et al., 2023). Furthermore, increasing temperatures are linked to heat-related mortality and morbidity, demanding time-sensitive policy interventions to protect the lives of the

most vulnerable (Argaud et al., 2007; Clark et al., 2024; Garcia et al., 2022; Kuehn, 2021; Kumar & Singh, 2021; Leon & Helwig, 2010).

IPUMS-NHGIS provides county-level climate summaries sourced from PRISM Climate Group data, from which I compile daily Tmax for all available years (1981-2014). For the period after 2014, I obtain daily Tmax raster files directly from the PRISM Climate Group (2015-2020). Processing these data in R, daily temperatures are aggregated to yearly averages, and then spatially aggregated to US counties using shapefiles. I then merge the Tmax values with the compiled IPUMS-NHGIS Tmax summaries, using year and county geographic identifier codes.

To complement the maximum air temperature metric, I use a wet bulb globe temperature (WBGT) heat stress index in my decomposition models. Beyond air temperature, the wet bulb metric captures the combined physiological effects of heat and humidity on the human body. The WBGT data (1981-2020) are derived from ERA5 reanalysis data produced by the European Centre for Medium-Range Weather Forecasts (ECMWF), and are calculated using dry bulb temperature, humidity, and surface pressure variables (5 km spatial resolution). Widely used in climate research to quantify exposure to heat-humidity conditions, WBGT provides a more direct indicator of physiological heat stress than ambient temperature alone, as high humidity constrains the body's ability to dissipate heat through the cooling process of sweating (Parsons et al., 2021). I therefore anticipate that incorporating a WBGT metric will allow this analysis to capture dimensions of heat exposure that may be underestimated by Tmax, particularly in areas where humid conditions amplify experiences of heat stress (Figure 1).[1] With these two metrics, I calculate 10-year means of Tmax and WBGT exposure to use in my analytical models.[2] These climate metrics (Tmax and WBGT) are then merged with the demographic data (IPUMS-NHGIS) using county geographic identifiers for place of residence at the time of the census (Table 1).

[1] For example, counties along the Gulf Coast—particularly in Louisiana and southeastern Texas—exhibit relatively moderate Tmax values compared to dry heat regions in the Southwest. These same counties, however, display distinctly higher WBGT measures. This contrast highlights how humid conditions can intensify environmental heat stress, even when ambient temperatures alone do not appear extreme.

[2] Averaging the metric values from the census year and the nine years prior.

FIGURE 1. County-level annual heat exposure across the United States: (A) Tmax in 1990, (B) Tmax in 2020, (C) WBGT in 1990, (D) WBGT in 2020

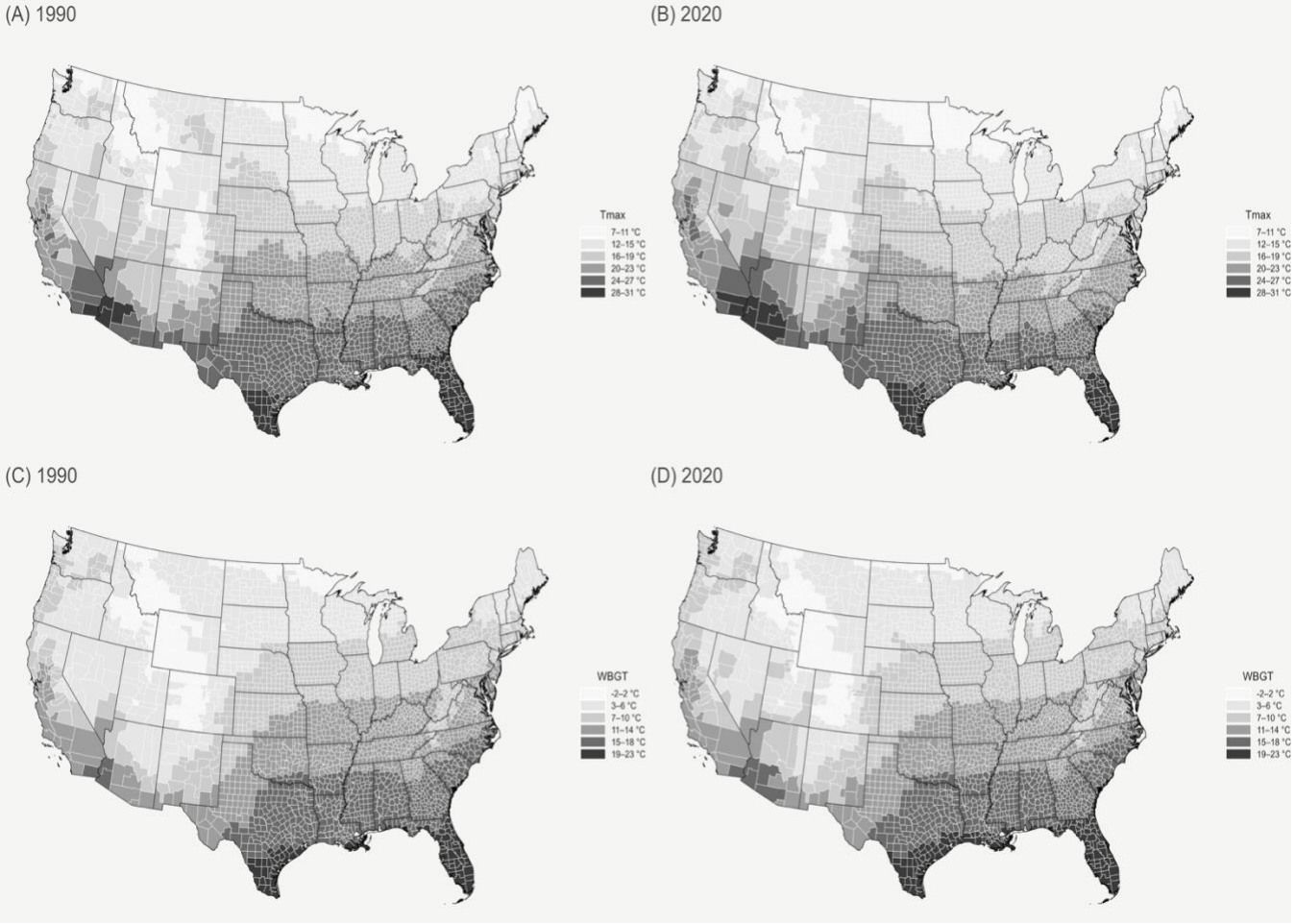

Table 1. Descriptive statistics

	Total population		Tmax observed exposure (°C)		WBGT observed exposure (°C)	
Year	Foreign-born	U.S.-born	Foreign-born	U.S.-born	Foreign-born	U.S.-born
1990	19,579,629	227,454,171	20.64	19.24	12.08	10.97
2000	30,858,381	248,714,468	20.82	19.37	12.37	11.27
2010	38,388,901	263,545,414	21.00	19.61	12.44	11.43
2020	43,808,614	280,603,630	21.25	19.97	12.94	11.95

Exposure is a 10-year average estimate of the temperature metric.
Tmax is maximum temperature. WBGT is wet bulb globe temperature.

Methods

I use decomposition methods to identify how much of an observed change in heat exposure is attributable to (1) changes in temperature and (2) shifts in population geographic distribution from 1990 to 2020. In the discipline of demography, decomposition is an analytical technique used to break down the change in an aggregate outcome (e.g., the crude morality rate) into components driven by variation in rates (e.g., age-specific mortality rates) and population composition (e.g., age structure) (Kitagawa, 1955; Shwartz et al., 2023). My decomposition approach estimates how different effects, temperature and population redistribution, individually contribute to the change in heat exposure over time.

The analysis follows four steps. First, I calculate the observed heat exposure by multiplying the local temperature by the proportion of the focal population of the given decennial year. Second, I sum these products across counties to obtain a population-weighted average temperature. Third, I generate counterfactual heat exposures. I hold weighted baseline population shares constant (e.g., 1990), while applying endline temperatures (e.g., 2020). Then I hold endline population shares constant (e.g., 2020), while applying weighted baseline temperatures (e.g., 1990). These counterfactual exposures are calculated using the same weighted averaging procedure (applied to find observed exposure). Finally, I decompose the total change in observed exposure into additive components: (1) a temperature effect, which estimates the average change in exposure that would occur if population distributions remained fixed, and (2) a population redistribution effect, which estimates the average change in exposure holding temperature constant. The temperature effect takes the form of:

$$\frac{1}{2}\left[\left(CE(P_{1990}, T_{2020}) - OE(P_{1990}, T_{1990})\right) + \left(OE(P_{2020}, T_{2020}) - CE(P_{2020}, T_{1990})\right)\right]$$

where *CE(P,T)* is the counterfactual exposure and *OE(P,T)* is the observed exposure for a given population *P* and temperature *T*.[3] The population redistribution effect then takes the form of:

$$\frac{1}{2}\left[\left(CE(P_{2020}, T_{1990}) - OE(P_{1990}, T_{1990})\right) + \left(OE(P_{2020}, T_{2020}) - CE(P_{1990}, T_{2020})\right)\right]$$

These calculations separate the total change in observed heat exposure into its temperature and population components, allowing identification of the dominant driver over time. As temperatures and populations shift simultaneously, these effects are not independent, making the simulation paths dependent. To address this, I calculate contributions in both directions—from 1990 to 2020 and from 2020 to 1990—and then compute the average of each (temperature and population) effect. This step of averaging is necessary because the observed change in heat exposure includes an interaction term (i.e., the product of the temperature and population components), and no single order of decomposition is uniquely correct. By evenly allocating for the interaction term, this additive decomposition approach accurately reflects the combined influence of both effects.

The decomposition models estimate heat exposure by nativity, and I begin by addressing two empirical questions: (1) What would the 1990 (non)immigrant population's heat exposure be under 2020 temperature conditions? (2) What would the 2020 (non)immigrant population's heat

[3] Subscripts denote census years.

exposure be under 1990 temperature conditions? The next set of simulations explore heterogeneity by metropolitan status, U.S. census divisions [4,5,6] (Figure 2), and foreign-born region of origin. For these subgroup analyses, population shares are calculated within each analytic subgroup rather than the total national population used in the overall nativity model. As subgroup classifications in IPUMS-NHGIS are not uniformly available across all census years, the population totals for metropolitan status, U.S. census divisions, and world region of origin are smaller than the total foreign- and US-born populations used in the main model. To conclude, I evaluate the robustness of my findings by conducting supplementary simulations using an alternative exposure period, later baseline year, and earlier endline year.

[4] To define county metropolitan status, I use the Rural-Urban Continuum Codes (RUCC) to ensure comparability across time and geographic units. Each county is consistently classified as metropolitan or nonmetropolitan for all models, supporting temporal comparisons (Cromartie & Bucholtz, 2008; Lichter & Johnson, 2009; Miller & Vasan, 2021). Developed by the U.S. Department of Agriculture's Economic Research Service (USDA ERS), RUCC are released approximately three years after each census (e.g., 2023 RUCC reflect data collected in the 2020 census) and classify counties based on population size and adjacency to metropolitan areas (U.S. Department of Agriculture, Economic Research Service 2024.

[5] RUCC codes 1 through 3 are metropolitan counties, based on the total population of their metropolitan area: 1 million+ (code 1), 250k to 1 million (code 2), below 250k (code 3). RUCC codes 4 through 9 are nonmetropolitan counties, based on the total urban population in the county: 20k+ (codes 4 and 5), 5k-20k (codes 6 and 7), fewer than 5k (codes 8 and 9). I create a binary variable where 1 equals metropolitan (RUCC 1-3) and 0 equals nonmetropolitan (RUCC 4-9).

[6] With my harmonization of county Federal Information Processing Standards (FIPS) codes across years, I address county name changes (e.g., Miami-Dade, Oglala Lakota) and county-equivalent restructuring in Connecticut to ensure consistent county-level identification across RUCC releases.

FIGURE 2. U.S. census divisions

Results

Overall estimates

My first model focuses on nativity-based differences in heat exposure, providing overall estimates of disparities between foreign- and native-born populations. Since 1990, the foreign-born have observed higher heat exposure compared to U.S.-born individuals, according to both air temperature (Tmax) and heat stress (WBGT) metrics (Figure 3). From 1990 to 2020, foreign-born exposure increased by approximately 0.61 °C (Tmax) and 0.86 °C (WBGT) (Table 1). Exposure among the native-born population increased by 0.72 °C (Tmax) and 0.98 °C (WBGT). While the U.S.-born experienced slightly larger increases in heat exposure since 1990, population-level heat disparities by nativity remain consistent, with immigrants experiencing higher levels of Tmax and WBGT exposure over time.

FIGURE 3. Heat exposure by nativity

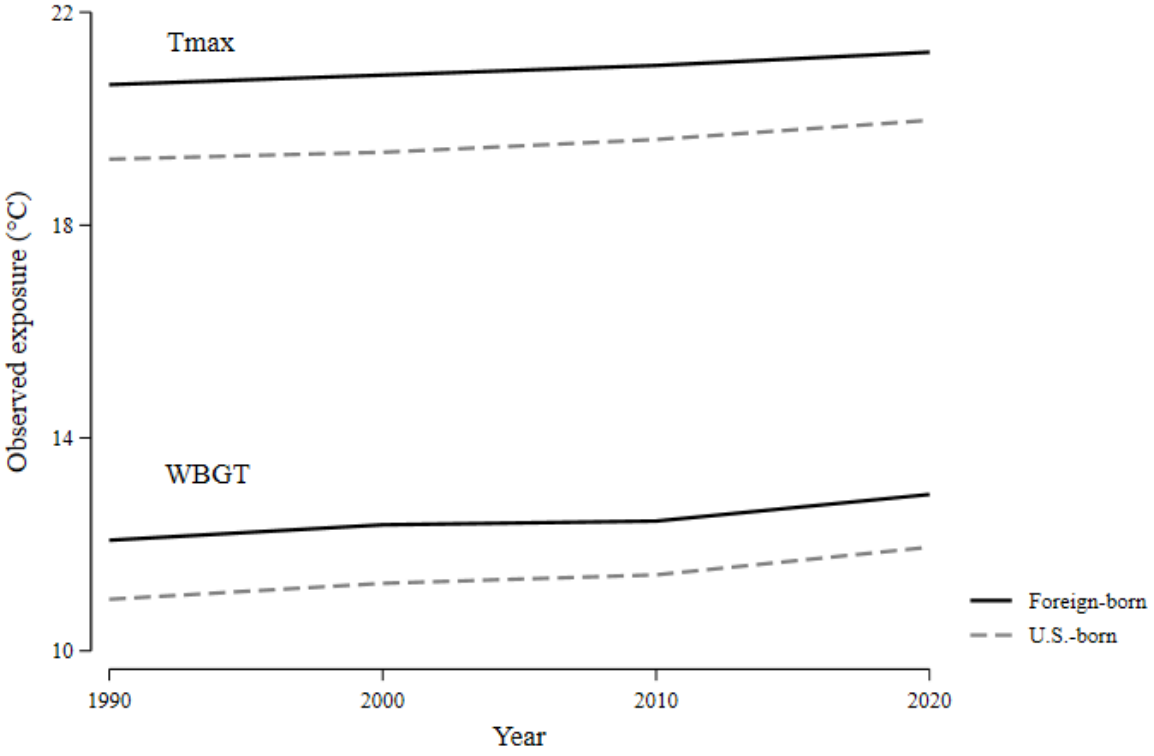

To interpret these observed exposures, I use demographic decomposition to break down the relative contributions of changing temperature and population redistribution effects by nativity status (Table 2). The combined impacts of these effects sum to a net effect, or in other words, the observed change in exposure between 1990 and 2020. According to the decomposition, I find that the 0.61 °C increase in foreign-born Tmax exposure is attributable to rising temperatures (0.29 °C, 48.45%) and a nearly equal population redistribution effect (0.31 °C, 51.55%) (Figure 4). Decomposition for the U.S.-born, however, show significantly different overall findings, with population redistribution (0.50 °C, 68.56%) playing a larger role than changing temperature (0.23 °C, 31.44%). These estimates suggest that increased Tmax exposure, regardless of population nativity, is shaped more by where people live, and less by shifts in air temperature.

Using WBGT in the decomposition shows results that differ substantially from those based on Tmax. For example, the 0.86 °C increase in foreign-born wet bulb exposure is driven more by a shift in temperature (0.58 °C, 67.56%) than by population redistribution (0.28 °C, 32.44%). Rising temperatures contribute more than 67 percent of the change in heat exposure, while population redistribution contributes roughly 32 percent. U.S.-born exposure additionally shows a dominant temperature effect (0.67 °C, 67.67%) compared to geographic distribution (0.32 °C, 32.33%), and these results indicate that heat disparities may be influenced more by environmental conditions (i.e., air temperature and humidity) than by where populations live.

Table 2. Decomposition of heat exposure, by nativity

	1990	2020	(1990 pop, 2020 temp)	(2020 pop, 1990 temp)		
	Observed exposure (°C)	Observed exposure (°C)	Counterfactual exposure (°C)	Counterfactual exposure (°C)	Temperature effect	Population redistribution effect
Foreign-born						
Tmax	20.64	21.25	20.94	20.96	0.29	0.31
WBGT	12.08	12.94	12.64	12.33	0.58	0.28
U.S.-born						
Tmax	19.24	19.97	19.46	19.73	0.23	0.50
WBGT	10.97	11.95	11.63	11.28	0.67	0.32

Exposure is a 10-year average estimate of the temperature metric.
Tmax is maximum temperature. WBGT is wet bulb globe temperature.

FIGURE 3. Heat exposure, by nativity

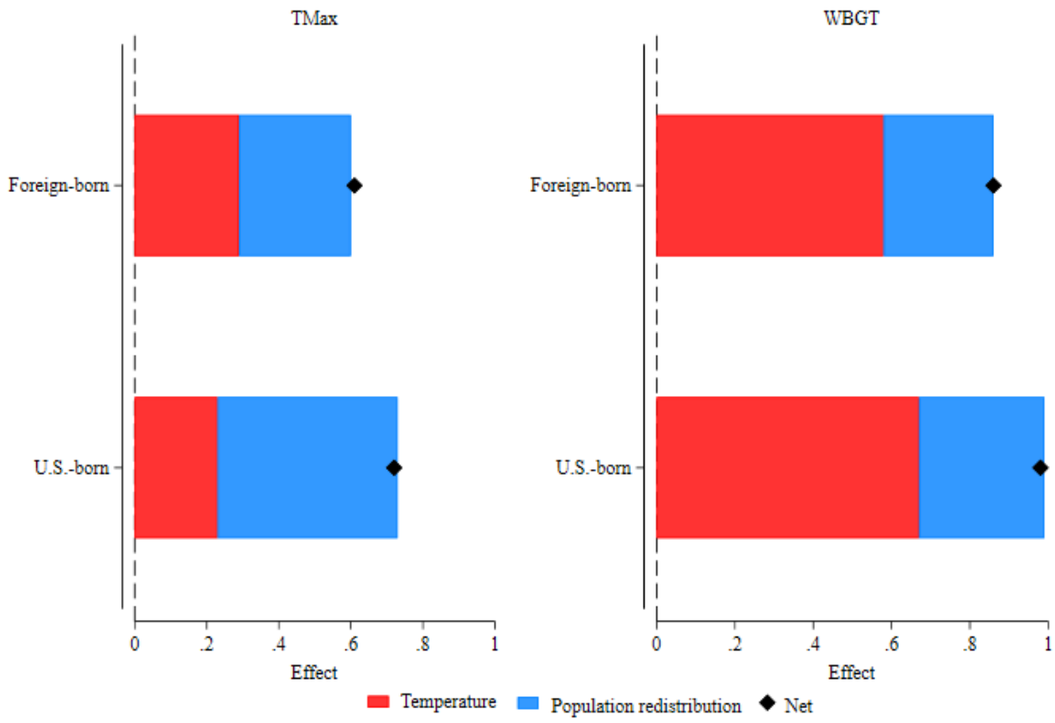

Spatial and demographic heterogeneity

The next set of analyses consider differences in heat exposure across demographic, geographic, and climatic profiles. I find that population redistribution accounts for over half of the increase in Tmax exposure among metropolitan (0.32 °C, 51.85%) and nonmetropolitan (0.46 °C, 60.19%) immigrants. Consistent with decomposition by nativity, rising air temperature contributes a relatively smaller impact on metropolitan (0.29 °C, 48.15%) and nonmetropolitan (0.30 °C, 39.81%) foreign-born populations (Table 2, Figure 4). Change in WBGT exposure, however, is driven by temperature effects. Among the foreign-born metropolitan, a 0.85 °C increase in heat exposure is largely attributable to rising temperatures (0.57 °C, 67.29%) and a smaller contribution from population redistribution (0.28 °C, 32.71%). Decomposition among the U.S.-born living in metropolitan counties show a qualitatively similar trend to their immigrant counterparts, with increased WBGT exposure primarily attributable to a temperature effect (0.66 °C, 65.57%). In contrast, the U.S.-born nonmetropolitan population fail to indicate a dominant temperature (0.15 °C, 52.37%) versus redistribution (0.14 °C, 48.63%) effect on the observed change in heat exposure. A large role, however, is displayed among foreign-born nonmetropolitan populations, where heat exposure is driven by an estimated 60 percent shift in population redistribution (0.46 °C, 60.19%), highlighting climate-related vulnerabilities in relation to the demographic trend of immigrants relocating to less populated rural counties.

Table 3. Decomposition of heat exposure, by metropolitan status

	1990	2020	1990 pop, 2020 temp	2020 pop, 1990 temp		
	Observed exposure (°C)	Observed exposure (°C)	Counterfactual exposure (°C)	Counterfactual exposure (°C)	Temperature effect	Population redistribution effect
Foreign-born						
Tmax						
Metropolitan	20.70	21.31	21.00	21.02	0.29	0.32
Nonmetropolitan	19.18	19.93	19.51	19.66	0.30	0.46
WBGT						
Metropolitan	12.16	13.01	12.70	12.41	0.57	0.28
Nonmetropolitan	10.34	11.54	11.01	10.84	0.68	0.52
U.S.-born						
Tmax						
Metropolitan	19.43	20.22	19.67	19.97	0.24	0.55
Nonmetropolitan	18.46	18.75	18.60	18.60	0.15	0.14
WBGT						
Metropolitan	11.16	12.16	11.81	11.50	0.66	0.35
Nonmetropolitan	10.17	10.96	10.87	10.26	0.70	0.09

Exposure is a 10-year average estimate of the temperature metric.
Tmax is maximum temperature. WBGT is wet bulb globe temperature.

FIGURE 4. Foreign-born heat exposure, by metropolitan status

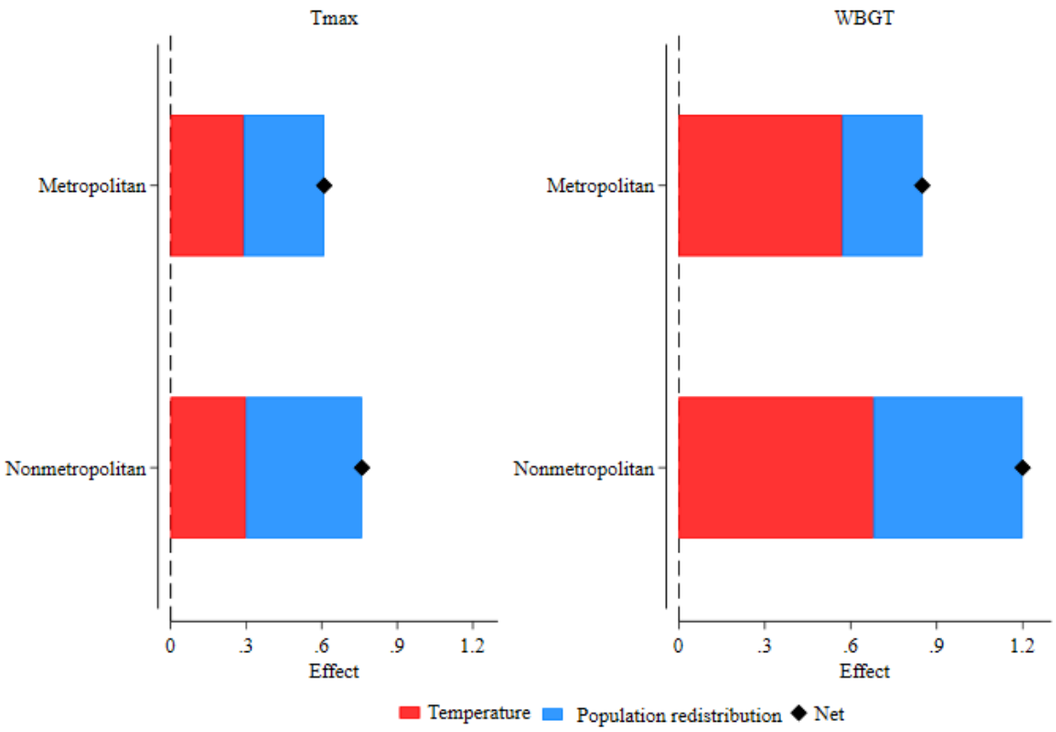

Next, I assess differences in heat exposure by the nine US census divisions located in the West (Pacific, Mountain), Midwest (West North Central, East North Central), Northeast (New England, Middle Atlantic) and South (West South Central, East South Central, South Atlantic) (Table 4). In the historically cooler Northeast, immigrants living in New England and the Middle Atlantic division both display an increase in Tmax exposure, attributable to rising temperatures in the two areas (Figure 5). Contributions of population redistribution, however, increase Tmax exposure for both divisions (West North Central and East North Central) in the Midwest. In the South—one of the nation's historically hottest regions—a decline in Tmax exposure is accountable to a negative population redistribution effect among foreign-born individuals in the East South Central and South Atlantic divisions. Higher air temperatures, however, primarily contribute to immigrant exposure for states like Texas in the West South Central division, an area with a large concentration of immigrants often working in outdoor industries (e.g., agriculture, construction). Counties in the West differ in their relative contributions to Tmax exposure, with population redistribution playing a larger role in the Pacific division and temperature driving a larger effect in the Mountain division.

Foreign-born WBGT exposure show less variation across census divisions. Temperature change is the primary driver of heat stress conditions in all census divisions, except where negative population redistribution occurs in the Pacific and South Atlantic. These WBGT exposure disparities found in Model 3 are consistent with the dominant temperate effects found in the nativity and metropolitan status WBGT results, revealing a clear pattern across demographic and spatial contexts.

In comparison to immigrant exposure, U.S.-born Tmax exposure reveals less variation. For instance, seven out of nine census divisions show a larger impact from temperature change, while the Mountain and South Atlantic display key contributions from the geographic distribution of the native population. U.S.-born WBGT exposure additionally supports the important role of rising temperatures across all census divisions.

Table 4. Decomposition of heat exposure, by US census divisions

	1990	2020	(1990 pop, 2020 temp)	(2020 pop, 1990 temp)		
	Observed exposure (°C)	Observed exposure (°C)	Counterfactual exposure (°C)	Counterfactual exposure (°C)	Temperature effect	Population redistribution effect
Foreign-born						
Tmax						
Pacific	22.33	22.16	22.65	21.85	0.32	-0.48
Mountain	22.06	22.78	22.59	22.30	0.51	0.21
West North Central	16.11	15.64	15.94	15.84	-0.19	-0.29
East North Central	15.11	15.23	15.12	15.21	0.02	0.11
New England	15.04	15.47	15.42	15.08	0.38	0.05
Middle Atlantic	16.49	16.88	16.82	16.53	0.34	0.05
West South Central	25.65	25.94	26.26	25.35	0.60	-0.31
East South Central	21.76	21.59	21.99	21.37	0.22	-0.40
South Atlantic	25.49	24.88	25.64	24.73	0.15	-0.76
WBGT						
Pacific	12.67	12.53	12.97	12.19	0.32	-0.46
Mountain	9.84	10.49	10.33	10.00	0.49	0.16
West North Central	7.89	8.27	8.47	7.68	0.59	-0.20
East North Central	7.93	8.55	8.44	8.03	0.52	0.10
New England	7.91	8.64	8.58	7.97	0.67	0.06
Middle Atlantic	9.23	9.99	9.92	9.28	0.70	0.06
West South Central	16.51	17.24	17.26	16.49	0.75	-0.02
East South Central	13.49	13.97	14.35	13.10	0.87	-0.39
South Atlantic	17.60	17.46	18.40	16.63	0.81	-0.96

Table 4. (Continued)

	1990 Observed exposure (°C)	2020 Observed exposure (°C)	(1990 pop, 2020 temp) Counterfactual exposure (°C)	(2020 pop, 1990 temp) Counterfactual exposure (°C)	Temperature effect	Population redistribution effect
U.S.-born						
Tmax						
Pacific	20.81	21.07	21.14	20.73	0.33	-0.08
Mountain	19.42	20.49	19.95	19.97	0.52	0.54
West North Central	16.23	16.02	16.05	16.21	-0.19	-0.03
East North Central	15.35	15.38	15.40	15.33	0.05	-0.02
New England	14.59	14.93	14.95	14.57	0.36	-0.02
Middle Atlantic	15.94	16.27	16.24	15.97	0.30	0.03
West South Central	24.66	25.26	25.10	24.80	0.46	0.15
East South Central	21.73	21.87	21.94	21.66	0.20	-0.07
South Atlantic	22.99	23.39	23.12	23.24	0.14	0.27
WBGT						
Pacific	11.34	11.59	11.73	11.20	0.39	-0.14
Mountain	7.85	8.73	8.36	8.22	0.51	0.37
West North Central	8.02	8.59	8.59	8.01	0.58	-0.01
East North Central	8.15	8.70	8.71	8.14	0.56	-0.01
New England	7.48	8.14	8.16	7.46	0.67	-0.02
Middle Atlantic	8.78	9.56	9.53	8.81	0.76	0.03
West South Central	15.85	16.72	16.59	15.97	0.74	0.12
East South Central	13.41	14.21	14.27	13.35	0.87	-0.06
South Atlantic	14.65	15.75	15.51	14.89	0.86	0.24

Table 4. (Continued)

Exposure is a 10-year average estimate of the temperature metric.
Tmax is maximum temperature. WBGT is wet bulb globe temperature.

FIGURE 5. Foreign-born heat exposure, by U.S. census divisions

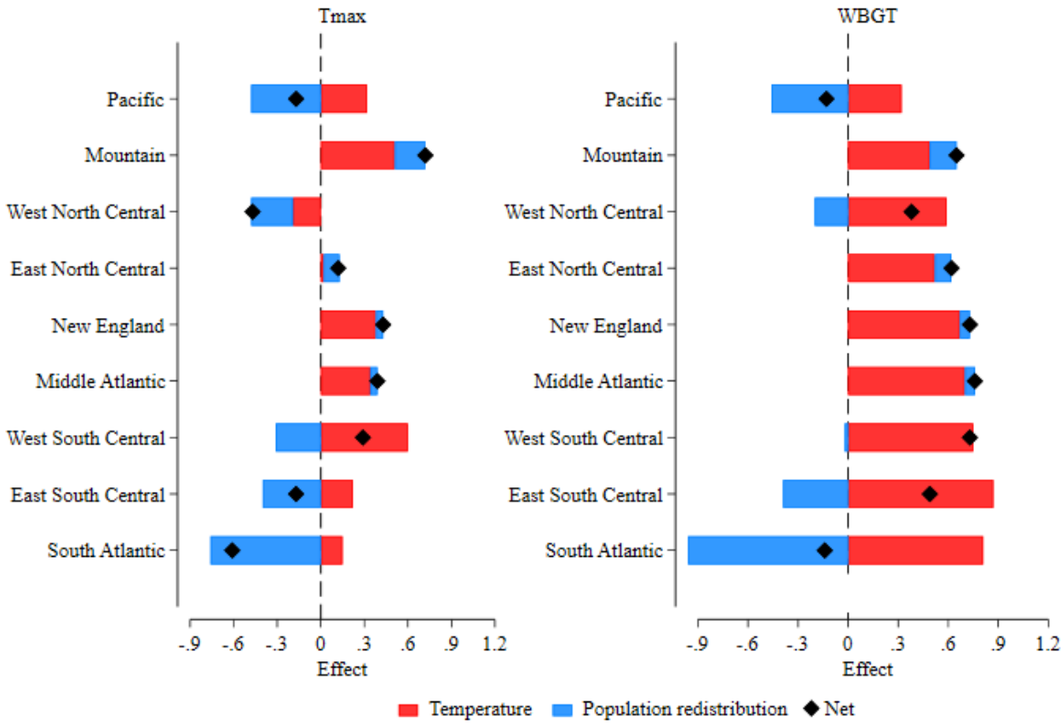

The last model explores demographic heterogeneity by world region of origin (Table 5). Immigrants born in the Americas and Asia show that temperature effects are the main contributor to changes in Tmax exposure (Figure 6). Population redistribution, however, account for most of the observed change in Tmax exposure for the remaining world regions of origin. Africa and Oceania interestingly reveal negative population redistribution effects, while in Europe a positive population redistribution effect (0.59 °C, 71.10%) contributes more to Tmax exposure than a smaller temperature effect (0.24 °C, 28.9%). WBGT results uniformly show the large role of temperature on immigrant exposure for all world regions of origin, consistent with the spatially disaggregated models.

Table 5. Decomposition of heat exposure, by world region of origin

	1990	2020	1990 pop, 2020 temp	2020 pop, 1990 temp		
	Observed exposure (°C)	Observed exposure (°C)	Counterfactual exposure (°C)	Counterfactual exposure (°C)	Temperature effect	Population redistribution effect
Foreign-born						
Tmax						
Africa	19.44	19.39	19.72	19.17	0.24	-0.30
Americas	22.02	22.42	22.37	22.09	0.34	0.06
Asia	20.01	20.28	20.27	20.03	0.26	0.01
Europe	18.50	19.34	18.75	19.10	0.24	0.59
Oceania	20.33	20.18	20.58	19.90	0.27	-0.41
WBGT						
Africa	11.25	11.62	11.90	10.93	0.66	-0.30
Americas	13.16	13.89	13.68	13.28	0.57	0.16
Asia	11.48	12.07	12.01	11.49	0.56	0.03
Europe	10.56	11.60	11.17	10.97	0.62	0.42
Oceania	11.43	11.62	11.96	11.05	0.55	-0.36

Exposure is a 10-year average estimate of the temperature metric.
Tmax is maximum temperature. WBGT is wet bulb globe temperature.

Figure 6. Heat exposure, by world region of origin

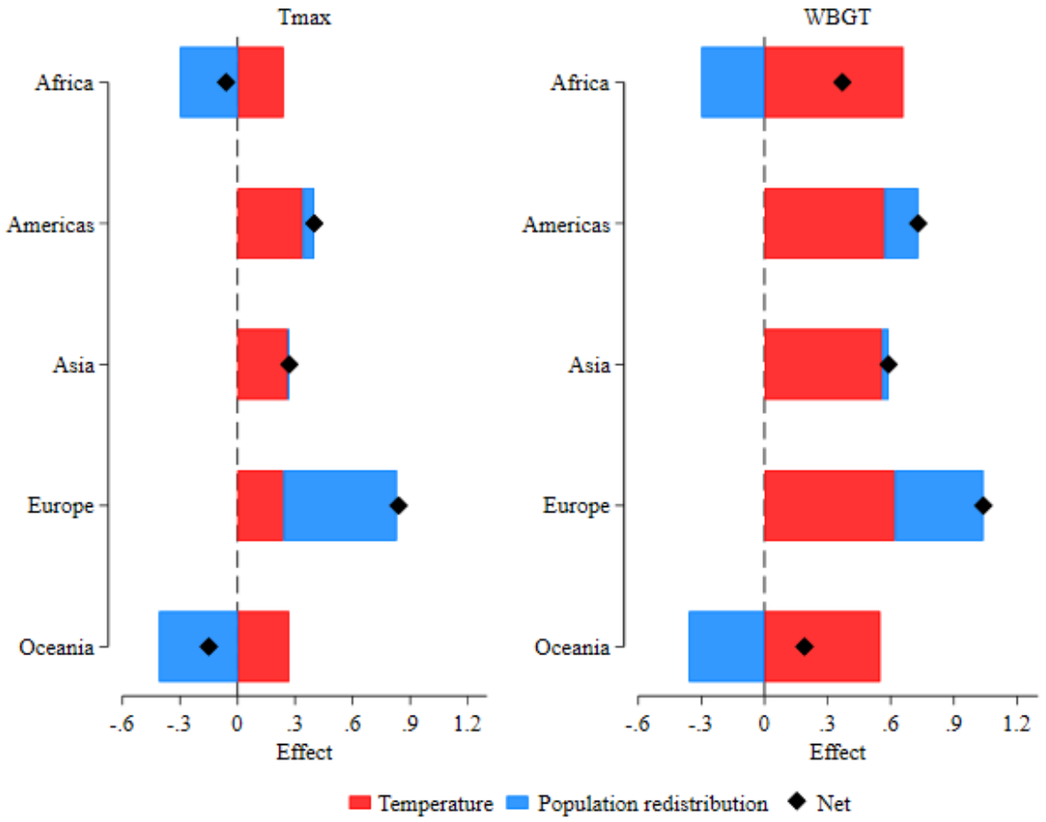

Robustness checks

Recognizing that the 10-year average exposure period is potentially contested, as longer temporal averaging windows may smooth meaningful short-term variation in heat exposure, I also fit decomposition models using a 5-year average exposure period (provided in appendix). In Model 1, I find that population redistribution largely contributes to Tmax exposure for both the foreign- and U.S.-born populations, and the same association is shown in the (Table S2) robustness check. Also consistent with the overall nativity model, WBGT exposure shows a dominant temperature effect in the robustness check. Overall supplementary simulations with later baseline and earlier endline years, however, reveals variation. Applying my decomposition methods to an earlier baseline model (2000 and 2020 exposure), immigrant exposure, using both metrics, is driven by rising temperatures (Table S3). Different from Model 1, this simulation specifically suggests that Tmax exposure is largely impacted by the role of air temperatures, and not population redistribution. Exploring a later endline year model (1990 to 2010 exposure), the geographic distribution of the immigrant population accounts for most of the observed change in heat exposure (Table S4), displaying a key shift from WBGT estimates previously linked to the impact of rising temperatures in Model 1.

Discussion and conclusion

Calculating the relative contributions of temperature change and population redistribution, this analysis measures changes in foreign- and U.S.-born heat exposure from 1990 to 2020. In addition to presenting overall exposure differences by nativity, I examine how the relative influence of temperature and population effects varies across smaller geographic contexts (U.S. census divisions) and subpopulation group characteristics (metropolitan status, region of origin). I find evidence that differences in heat exposure are linked to both temperature and population effects, with their relative contributions varying by county geographic, demographic, and climatic profiles.

The results point to four main takeaways. First, immigrants experience higher heat exposure than the U.S.-born population, but the dominant driver of change in exposure depends on the temperature metric used. For example, decomposition by nativity shows that Tmax exposure is largely attributable to a population redistribution effect, suggesting that shifts in where people live play a greater role than uniform warming alone. In contrast, change in WBGT exposure is driven more by rising temperatures, indicating that environmental heat stress conditions have intensified across U.S. counties over time. This contrast in results likely reflects the composite structure of WBGT, which incorporates humidity, solar radiation, and wind speed in addition to air temperature, arguably making it more sensitive to changes in the broader

atmospheric environment than Tmax alone. Overall, the nativity model suggests that Tmax captures geographic into warmer locations, whereas WBGT captures changes in local heat stress conditions that are not solely explained by population redistribution.

Second, regional differences in exposure reveal that foreign-born heat vulnerability across the US is spatially uneven, and metric dependent. Decomposition results show increasing Tmax exposure in historically cooler divisions (e.g., New England, Middle Atlantic), where increases are largely driven by temperature change, aligning with previous decomposition studies documenting emerging heat-related risks in the Northeast (Carr, 2024). In contrast, several southern divisions display declining Tmax exposure among immigrants, primarily due to negative population redistribution effects, potentially suggesting shifts away from some of the hottest counties in the nation. WBGT results, however, present a more consistent regional pattern across nearly all census divisions, with temperature change as the main contributor to rising heat stress. This key takeaway suggests that while exposure to Tmax air temperature reflects region-specific demographic change, WBGT exposure captures broader shifts in environmental heat stress across the diverse climatic zones of census divisions. Together, these findings support prior evidence that heat burdens in the US are not uniformly distributed across space (Jones et al., 2015; Tuholske et al., 2021), and underscore the importance of regionally tailored adaptive strategies and early warning systems designed to address the distinct role of climatic and demographic contributions to heat exposure.

Third, drivers of exposure vary by immigrant subpopulations, specifically by metropolitan status and world region of origin, highlighting important demographic heterogeneity in heat disparities. For Tmax, population redistribution plays a large role for many immigrant groups, including metropolitan and nonmetropolitan populations and for several world regions of origin. This finding suggests that mobility and settlement patterns, often influenced by local labor markets, likely impact exposure to air temperatures. Changes in WBGT conditions, however, are consistently explained by temperature effects across metropolitan contexts and all world regions of origin. This pattern suggests that diverse immigrant groups are increasingly exposed to physiologically relevant heat stress. In all, my Tmax and WBGT results highlight the need for targeted interventions that account for both place-based vulnerabilities and differences in sociodemographic risk profiles.

Fourth, while shifts in temperature and the geographic distribution of foreign- and U.S.-born populations directly influence heat disparities, the underlying mechanisms of population change remain unclear. In this analysis, population change captures both net migration and natural increase (i.e., the difference between births and deaths), but data limitations prevent deeper insight into the factors shaping these patterns and their association with higher or lower heat exposure. Migration, for example, may increase exposure if certain immigrant groups relocate to warmer metropolitan areas for employment opportunities and (or) to avoid cold stress (Ruther et al., 2018; Scott et al., 2005). At the same time, regional variation in mortality and fertility across immigrant groups may alter the demographic composition of local communities, thereby influencing aggregate heat exposure independent of migration. As an example, higher mortality among older foreign-born residents could shift the age composition of a US county, potentially affecting the distribution of temperature-sensitive populations and overall exposure levels (Noghanibehambari & Fletcher, 2025; Shor & Roelfs, 2019; Obolensky et al., 2024; Sidney et al., 2025; Mercereau et al., 2017). Selective return migration and climate-related mobility may additionally contribute to population change dynamics. Therefore, as demographic processes (migration, fertility, mortality) likely interact, additional data are needed to clarify how the role of these factors impact population change to better inform effective heat policies.

Thes findings contribute to the decomposition literature on climate warming and population vulnerability to heat (Carr, 2024, Park et al., 2020; Tuholske et al., 2021), but several limitations of this study should be addressed in future research. For instance, as the census primarily collects fundamental demographic information, limited detail on social and economic variables restricts my ability to examine additional sources of heterogeneity that may play a role in heat exposure. More specifically, this data limitation restricts modeling short-term migration histories, timing and causes of mortality, and other demographic processes. Consequently, analyzing changes in exposure over ten-year intervals provides a relatively coarse evaluation of spatial and demographic heterogeneity. Furthermore, critical dimensions of heat vulnerability (e.g., access to cooling infrastructure, outdoor labor participation) are also not captured in the NHGIS data, potentially overlooking critical factors influencing population-level disparities.

With limitations such as these, future studies would benefit from more detailed data and the exploration of other demographic-related factors. For one, more research is needed on the motivations behind residential (im)mobility. My findings show that temperature and population shifts occur simultaneously, yet the reasons behind relocation to cooler or hotter areas remain

unclear. This analysis additionally underscores the need to examine linkages between temperature change and population redistribution across a wider range of subpopulation groups. I identify variation in the primary driver of exposure by geographic localities (metropolitan status, census divisions) and world region of birth, yet other individual- (e.g., educational attainment) and household-level (e.g., income, immigrant-native intermarriage or co-residence) characteristics may also impact heat exposure (Ellis & Wright, 2005; Slesinski et al., 2025). Future research should decompose the change in exposure by relevant group stratifications to assess whether and how social and structural disadvantages heighten heat-related risks. Given variation in exposure by nativity, more research attention to generational differences may also enhance our understanding of heat disparities. Beyond the comparison between foreign- and U.S.-born populations, future studies might investigate differences in heat exposure among second and third generation immigrants.

In conclusion, this analysis demonstrates the utility of demographic decomposition by revealing that temperature change and population redistribution both contribute to observed changes in foreign- and U.S.-born heat exposure. Evidence on the relative contributions of these effects is essential for assessing differential heat risks across demographic groups and regions, and this knowledge can inform more effective and equitable heat mitigation policies in the United States. In all, decomposition provides a critical tool for separating the contributions of demographic and climatic factors driving heat exposure, guiding evidence-based interventions to protect vulnerable populations.

References

Ahn, Y., Tuholske, C., & Parks, R. M. (2024). Comparing Approximated Heat Stress Measures Across the United States. *GeoHealth*, *8*(1), e2023GH000923. https://doi.org/10.1029/2023GH000923

Albouy, D., Graf, W., Kellogg, R., & Wolff, H. (2016). Climate Amenities, Climate Change, and American Quality of Life. *Journal of the Association of Environmental and Resource Economists*, *3*(1), 205–246. https://doi.org/10.1086/684573

Argaud, L., Ferry, T., Le, Q.-H., Marfisi, A., Ciorba, D., Achache, P., Ducluzeau, R., & Robert, D. (2007). Short- and Long-term Outcomes of Heatstroke Following the 2003 Heat Wave in Lyon, France. *Archives of Internal Medicine*, *167*(20), 2177–2183. https://doi.org/10.1001/archinte.167.20.ioi70147

Burton, L. M., Lichter, D. T., Baker, R. S., & Eason, J. M. (2013). Inequality, Family Processes, and Health in the "New" Rural America. *American Behavioral Scientist*, *57*(8), 1128–1151. https://doi.org/10.1177/0002764213487348

Calvin, K., Dasgupta, D., Krinner, G., Mukherji, A., Thorne, P. W., Trisos, C., Romero, J., Aldunce, P., Barrett, K., Blanco, G., Cheung, W. W. L., Connors, S., Denton, F., Diongue-Niang, A., Dodman, D., Garschagen, M., Geden, O., Hayward, B., Jones, C., … Péan, C. (2023). *IPCC, 2023: Climate Change 2023: Synthesis Report. Contribution of Working Groups I, II and III to the Sixth Assessment Report of the Intergovernmental Panel on Climate Change [Core Writing Team, H. Lee and J. Romero (eds.)]. IPCC, Geneva, Switzerland.* (First). Intergovernmental Panel on Climate Change (IPCC). https://doi.org/10.59327/IPCC/AR6-9789291691647

Carr, D., Falchetta, G., & Sue Wing, I. (2024). Population Aging and Heat Exposure in the 21st Century: Which U.S. Regions Are at Greatest Risk and Why? *The Gerontologist*, *64*(3), gnad050. https://doi.org/10.1093/geront/gnad050

Clark, A., Grineski, S., Curtis, D. S., & Cheung, E. S. L. (2024). Identifying groups at-risk to extreme heat: Intersections of age, race/ethnicity, and socioeconomic status. *Environment International*, *191*, 108988. https://doi.org/10.1016/j.envint.2024.108988

Clay, L. A., Slotter, R., Heath, B., Lange (Leach), V., & Colón-Ramos, U. (2021). Capturing Disruptions to Food Availability After Disasters: Assessing the Food Environment Following Hurricanes Florence and María. *Disaster Medicine and Public Health Preparedness*, 1–8. https://doi.org/10.1017/dmp.2021.145

Cromartie, J., & Bucholtz, S. (2008, June 1). *Defining the "Rural" in Rural America | Economic Research Service*. https://www.ers.usda.gov/amber-waves/2008/june/defining-the-rural-in-rural-america

Crowley, M., Lichter, D. T., & Turner, R. N. (2019). *Diverging fortunes? Economic well-being of Latinos and African Americans in new rural destinations—ScienceDirect*. https://www.sciencedirect.com/science/article/pii/S0049089X14002038?casa_token=JwgUBME7MzAAAAAA:iTz5nlMsiF_LaI5XQN8FJFOQUovQji8XNvTcGroEiLQ4tcvv1Ac58LFCrobwTR5a1jozfrPl

DeVine, A. C., Vu, P. T., Yost, M. G., Seto, E. Y. W., & Busch Isaksen, T. M. (2017). A Geographical Analysis of Emergency Medical Service Calls and Extreme Heat in King County, WA, USA (2007–2012). *International Journal of Environmental Research and Public Health*, *14*(8), Article 8. https://doi.org/10.3390/ijerph14080937

Ellis, M., & Wright, R. (2005). Assimilation and differences between the settlement patterns of individual immigrants and immigrant households. *Proceedings of the National Academy of Sciences*, *102*(43), 15325–15330. https://doi.org/10.1073/pnas.0507310102

FitzGerald, D. S. (2022). The Sociology of International Migration. In *Migration Theory* (4th ed.). Routledge.

Flippen, C. A., & Farrell-Bryan, D. (2021). New Destinations and the Changing Geography of Immigrant Incorporation. *Annual Review of Sociology*, *47*(Volume 47, 2021), 479–500. https://doi.org/10.1146/annurev-soc-090320-100926

Fong, K. C., Heo, S., Lim, C. C., Kim, H., Chan, A., Lee, W., Stewart, R., Choi, H. M., Son, J.-Y., & Bell, M. L. (2022). The Intersection of Immigrant and Environmental Health: A Scoping Review of Observational Population Exposure and Epidemiologic Studies. *Environmental Health Perspectives*, *130*(9), 096001. https://doi.org/10.1289/EHP9855

Frey, W. H., Liaw, K.-L., & Wright, R. (2005). Migration within the United States: Role of Race-Ethnicity [with Comments]. *Brookings-Wharton Papers on Urban Affairs*, 207–262.

Garcia, C. K., Renteria, L. I., Leite-Santos, G., Leon, L. R., & Laitano, O. (2022). Exertional heat stroke: Pathophysiology and risk factors. *BMJ Medicine*, *1*(1), e000239. https://doi.org/10.1136/bmjmed-2022-000239

Hall, M., & Crowder, K. (2014). Native Out-Migration and Neighborhood Immigration in New Destinations. *Demography*, *51*(6), 2179–2202. https://doi.org/10.1007/s13524-014-0350-5

Hall, M., & Greenman, E. (2015). The Occupational Cost of Being Illegal in the United States: Legal Status, Job Hazards, and Compensating Differentials. *International Migration Review*, *49*(2), 406–442. https://doi.org/10.1111/imre.12090

Jensen, L., Monnat, S. M., Green, J. J., Hunter, L. M., & Sliwinski, M. J. (2020). Rural Population Health and Aging: Toward a Multilevel and Multidimensional Research Agenda for the 2020s. *American Journal of Public Health*, *110*(9), 1328–1331. https://doi.org/10.2105/AJPH.2020.305782

Jessoe, K., Manning, D. T., & Taylor, J. E. (2018). Climate Change and Labour Allocation in Rural Mexico: Evidence from Annual Fluctuations in Weather. *The Economic Journal*, *128*(608), 230–261. https://doi.org/10.1111/ecoj.12448

Johnson, K. M., & Lichter, D. T. (2019). Rural Depopulation: Growth and Decline Processes over the Past Century. *Rural Sociology*, *84*(1), 3–27. https://doi.org/10.1111/ruso.12266

Johnson, K. M., & Winkler, R. L. (2015). Migration signatures across the decades: Net migration by age in U.S. counties, 1950-2010. *Demographic Research*, *32*, 1065–1080. https://doi.org/10.4054/DemRes.2015.32.38

Jones, B., O'Neill, B. C., McDaniel, L., McGinnis, S., Mearns, L. O., & Tebaldi, C. (2015). Future population exposure to US heat extremes. *Nature Climate Change*, *5*(7), 652–655. https://doi.org/10.1038/nclimate2631

Jones, T. S., Liang, A. P., Kilbourne, E. M., Griffin, M. R., Patriarca, P. A., Wassilak, S. G. F., Mullan, R. J., Herrick, R. F., Donnell, H. D., Jr, Choi, K., & Thacker, S. B. (1982). Morbidity and Mortality Associated With the July 1980 Heat Wave in St Louis and Kansas City, Mo. *JAMA*, *247*(24), 3327–3331. https://doi.org/10.1001/jama.1982.03320490025030

Karl, T. R., & Quayle, R. G. (1981). *The 1980 Summer Heat Wave and Drought in Historical Perspective*. https://journals.ametsoc.org/view/journals/mwre/109/10/1520-0493_1981_109_2055_tshwad_2_0_co_2.xml

Kitagawa, E. M. (1955). Components of a Difference Between Two Rates*. *Journal of the American Statistical Association*, *50*(272), 1168–1194. https://doi.org/10.1080/01621459.1955.10501299

Kuehn, B. M. (2021). Why Farmworkers Need More Than New Laws for Protection From Heat-Related Illness. *JAMA*, *326*(12), 1135–1137. https://doi.org/10.1001/jama.2021.15454

Kumar, A., & Singh, D. P. (2021). Heat stroke-related deaths in India: An analysis of natural causes of deaths, associated with the regional heatwave. *Journal of Thermal Biology*, *95*, 102792. https://doi.org/10.1016/j.jtherbio.2020.102792

Leon, L. R., & Helwig, B. G. (2010). Heat stroke: Role of the systemic inflammatory response. *Journal of Applied Physiology*, *109*(6), 1980–1988. https://doi.org/10.1152/japplphysiol.00301.2010

Lichter, D. T., & Johnson, K. M. (2009). Immigrant Gateways and Hispanic Migration to New Destinations. *International Migration Review*, *43*(3), 496–518. https://doi.org/10.1111/j.1747-7379.2009.00775.x

Mercereau, L., Todd, N., Rey, G., & Valleron, A.-J. (2017). Comparison of the temperature-mortality relationship in foreign born and native born died in France between 2000 and 2009. *International Journal of Biometeorology*, *61*(10), 1873–1884. https://doi.org/10.1007/s00484-017-1373-6

Miller, C. E., & Vasan, R. S. (2021). The southern rural health and mortality penalty: A review of regional health inequities in the United States. *Social Science & Medicine*, *268*, 113443. https://doi.org/10.1016/j.socscimed.2020.113443

Moyce, S. C., & Schenker, M. (2018). Migrant Workers and Their Occupational Health and Safety. *Annual Review of Public Health*, *39*(Volume 39, 2018), 351–365. https://doi.org/10.1146/annurev-publhealth-040617-013714

Namias, J. (1982). *Anatomy of Great Plains Protracted Heat Waves (especially the 1980 U.S. summer drought)*. https://journals.ametsoc.org/view/journals/mwre/110/7/1520-0493_1982_110_0824_aogpph_2_0_co_2.xml

Nawrotzki, R. J., & DeWaard, J. (2016). Climate shocks and the timing of migration from Mexico. *Population and Environment*, *38*(1), 72–100. https://doi.org/10.1007/s11111-016-0255-x

Nawrotzki, R. J., Hunter, L. M., Runfola, D. M., & Riosmena, F. (2015). Climate change as a migration driver from rural and urban Mexico. *Environmental Research Letters*, *10*(11), 114023. https://doi.org/10.1088/1748-9326/10/11/114023

Nawrotzki, R. J., Riosmena, F., & Hunter, L. M. (2013). Do Rainfall Deficits Predict U.S.-Bound Migration from Rural Mexico? Evidence from the Mexican Census. *Population Research and Policy Review*, *32*(1), 129–158. https://doi.org/10.1007/s11113-012-9251-8

Noghanibehambari, H., & Fletcher, J. (2025). Chilling Sunsets: Climate Distances and Later-Life Mortality of Immigrants. *Environmental and Resource Economics*. https://doi.org/10.1007/s10640-025-01026-5

Nori-Sarma, A., Sun, S., Sun, Y., Spangler, K. R., Oblath, R., Galea, S., Gradus, J. L., & Wellenius, G. A. (2022). Association Between Ambient Heat and Risk of Emergency Department Visits for Mental Health Among US Adults, 2010 to 2019. *JAMA Psychiatry*, *79*(4), 341–349. https://doi.org/10.1001/jamapsychiatry.2021.4369

Obolensky, M., Tabellini, M., & Taylor, C. (2024). *Migration, Climate Similarity, and the Consequences of Climate Mismatch* (Working Paper No. 32035). National Bureau of Economic Research. https://doi.org/10.3386/w32035

Park, C.-E., Jeong, S., Harrington, L. J., Lee, M.-I., & Zheng, C. (2020). Population ageing determines changes in heat vulnerability to future warming. *Environmental Research Letters*, *15*(11), 114043. https://doi.org/10.1088/1748-9326/abbd60

Ruther, M., Tesfai, R., & Madden, J. (2018). Foreign-born population concentration and neighbourhood growth and development within US metropolitan areas. *Urban Studies*, *55*(4), 826–843. https://doi.org/10.1177/0042098016672804

Scott, D. M., Coomes, P. A., & Izyumov, A. I. (2005). The Location Choice of Employment-based Immigrants among U.S. Metro Areas. *Journal of Regional Science*, *45*(1), 113–145. https://doi.org/10.1111/j.0022-4146.2005.00366.x

Shor, E., & Roelfs, D. (2019). Climate shock: Moving to colder climates and immigrant mortality. *Social Science & Medicine*, *235*, 112397. https://doi.org/10.1016/j.socscimed.2019.112397

Shroeder, J., Van Riper, D., Manson, S., Knowles, K., Kugler, T., Roberts, F., & Ruggles, S. (2025). *IPUMS National Historical Geographic Information System: Version 20.0* (Version 20.0) [Dataset]. http://doi.org/10.18128/D050.V20.0

Shwartz, M., Rosen, A. K., Beilstein-Wedel, E., Davila, H., Harris, A. H., & Gurewich, D. (2023). Using the Kitagawa Decomposition to Measure Overall—and Individual Facility Contributions to—Within-facility and Between-facility Differences: Analyzing Racial and Ethnic Wait Time Disparities in the Veterans Health Administration. *Medical Care*, *61*(6), 392. https://doi.org/10.1097/MLR.0000000000001849

Sidney, B. T., Chandras, S., Campbell, S. M., Salma, J., & Yamamoto, S. S. (2025). Health-related impacts of climate change and air pollution on older adult, child, and adolescent immigrants and refugees globally: A scoping review. *Journal of Public Health*, *33*(6), 1341–1349. https://doi.org/10.1007/s10389-023-02103-z

Slesinski, S. C., Matthies-Wiesler, F., Breitner-Busch, S., Gussmann, G., & Schneider, A. (2025). Social inequalities in exposure to heat stress and related adaptive capacity: A systematic review. *Environmental Research Letters*, *20*(3), 033005. https://doi.org/10.1088/1748-9326/adb509

Spangler, K. R., Weinberger, K. R., & Wellenius, G. A. (2019). Suitability of gridded climate datasets for use in environmental epidemiology. *Journal of Exposure Science & Environmental Epidemiology*, *29*(6), 777–789. https://doi.org/10.1038/s41370-018-0105-2

Taylor, E. V., Vaidyanathan, A., Flanders, W. D., Murphy, M., Spencer, M., & Noe, R. S. (2018, April 26). *Differences in Heat-Related Mortality by Citizenship Status: United States, 2005–2014* (world) [Research-article]. Https://Doi.Org/10.2105/AJPH.2017.304006; American Public Health Association. https://doi.org/10.2105/AJPH.2017.304006

Tuholske, C., Caylor, K., Funk, C., Verdin, A., Sweeney, S., Grace, K., Peterson, P., & Evans, T. (2021). Global urban population exposure to extreme heat. *Proceedings of the National Academy of Sciences*, *118*(41), e2024792118. https://doi.org/10.1073/pnas.2024792118

Winkler, R. L., & Rouleau, M. D. (2021). Amenities or disamenities? Estimating the impacts of extreme heat and wildfire on domestic US migration. *Population and Environment*, *42*(4), 622–648. https://doi.org/10.1007/s11111-020-00364-

Appendix

Table S1. Descriptive statistics

	Total population		Tmax observed exposure (°C)		WBGT observed exposure (°C)	
Year	Foreign-born	U.S.-born	Foreign-born	U.S.-born	Foreign-born	U.S.-born
1990	19,579,629	227,454,171	20.80	19.48	12.15	11.12
2000	30,858,381	248,714,468	20.87	19.47	12.38	11.30
2010	38,388,901	263,545,414	21.04	19.63	12.36	11.36
2020	43,808,614	280,603,630	21.27	20.05	13.18	12.21

Exposure is a 5-year average estimate of the temperature metric.
Tmax is maximum temperature. WBGT is wet bulb globe temperature.

Table S2. Decomposition of heat exposure, by nativity

	1990	2020	(1990 pop, 2020 temp)	(2020 pop, 1990 temp)		
	Observed exposure (°C)	Observed exposure (°C)	Counterfactual exposure (°C)	Counterfactual exposure (°C)	Temperature effect	Population redistribution effect
Foreign-born						
Tmax	20.80	21.27	20.93	21.15	0.13	0.35
WBGT	12.15	13.18	12.86	12.43	0.72	0.30
U.S.-born						
Tmax	19.48	20.05	19.55	19.98	0.07	0.50
WBGT	11.12	12.21	11.89	11.43	0.77	0.32

Exposure is a 10-year average estimate of the temperature metric.
Tmax is maximum temperature. WBGT is wet bulb globe temperature.

Table S2. Decomposition of heat exposure, by nativity

	2000	2020	(2000 pop, 2020 temp)	(2020 pop, 2000 temp)		
	Observed exposure (°C)	Observed exposure (°C)	Counterfactual exposure (°C)	Counterfactual exposure (°C)	Temperature effect	Population redistribution effect
Foreign-born						
Tmax	20.82	21.25	21.09	20.98	0.27	0.16
WBGT	12.37	12.94	12.74	12.55	0.38	0.19
U.S.-born						
Tmax	19.37	19.97	19.63	19.71	0.25	0.34
WBGT	11.27	11.95	11.73	11.49	0.47	0.22

Exposure is a 10-year average estimate of the temperature metric.
Tmax is maximum temperature. WBGT is wet bulb globe temperature.

Table S3. Decomposition of heat exposure, by nativity

	1990	2010	(1990 pop, 2010 temp)	(2010 pop, 1990 temp)		
	Observed exposure (°C)	Observed exposure (°C)	Counterfactual exposure (°C)	Counterfactual exposure (°C)	Temperature effect	Population redistribution effect
Foreign-born						
Tmax	20.64	21.00	20.70	20.93	0.07	0.29
WBGT	12.08	12.44	12.24	12.26	0.17	0.19
U.S.-born						
Tmax	19.24	19.61	19.29	19.56	0.05	0.32
WBGT	10.97	11.43	11.23	11.17	0.27	0.20

Exposure is a 10-year average estimate of the given metric.
Tmax is maximum temperature. WBGT is wet bulb globe temperature.

Table S5. Descriptive statistics

	1990	2020
	Total population	Total population
U.S. census divisions		
Foreign-born		
Pacific	6,920,276	11,963,345
Mountain	714,912	2,678,310
West North Central	348,145	1,311,293
East North Central	1,783,148	3,649,443
New England	1,043,237	1,987,827
Mid Atlantic	4,187,787	7,281,892
West South Central	1,702,199	5,401,947
East South Central	157,149	760,973
South Atlantic	2,722,776	8,773,584
U.S.-born		
Pacific	30,548,758	39,071,489
Mountain	12,943,812	21,856,641
West North Central	17,311,545	20,039,219
East North Central	40,225,794	43,219,771
New England	12,163,706	12,833,932
Mid Atlantic	33,414,499	33,913,260
West South Central	25,000,594	34,859,326
East South Central	15,019,135	18,348,268
South Atlantic	40,826,328	56,461,724
Metropolitan status		
Foreign-born		
Metropolitan	18,804,653	41,791,390
Nonmetropolitan	774,976	2,010,261
U.S.-born		
Metropolitan	184,000,000	232,100,000
Nonmetropolitan	43,504,171	48,443,373
World region of origin		
Foreign-born		
Africa	362,894	2,358,305
Asia	4,833,859	13,561,490
Americas	9,148,376	22,870,600
Europe	4,336,113	4,765,290
Oceania	95,459	252,421